

Numerical simulation of vortical ideal fluid flow through curved channel

N. P. Moshkin^{1,*},† and P. Mounnamprang²

¹*School of Mathematics, Suranaree University of Technology, Nakhon Ratchasima, Thailand*

²*Rajabhat Petchburiwittayalongkorn Institute, Pathumthani, Thailand*

SUMMARY

A numerical algorithm to study the boundary-value problem in which the governing equations are the steady Euler equations and the vorticity is given on the inflow parts of the domain boundary is developed. The Euler equations are implemented in terms of the stream function and vorticity. An irregular physical domain is transformed into a rectangle in the computational domain and the Euler equations are rewritten with respect to a curvilinear co-ordinate system. The convergence of the finite-difference equations to the exact solution is shown experimentally for the test problems by comparing the computational results with the exact solutions on the sequence of grids. To find the pressure from the known vorticity and stream function, the Euler equations are utilized in the Gromeka–Lamb form. The numerical algorithm is illustrated with several examples of steady flow through a two-dimensional channel with curved walls. The analysis of calculations shows strong dependence of the pressure field on the vorticity given at the inflow parts of the boundary. Plots of the flow structure and isobars, for different geometries of channel and for different values of vorticity on entrance, are also presented. Copyright © 2003 John Wiley & Sons, Ltd.

KEY WORDS: flowing through problem; ideal incompressible fluid flow; finite-difference scheme

1. INTRODUCTION

A flow of an ideal incompressible liquid through the given region rather interesting for its applications, for a long time remained not investigated. The problem of fluid motion in a given domain whose boundaries do not only consist of solid impermeable parts but also include the inflow and outflow parts we will call the ‘flowing-through’ problem.

The proof that the boundary-value problem for the Euler equations of an ideal fluid is well posed, is quite difficult even for the problem considered in small time intervals. Sufficiently complete results have been obtained in the case where fluid motion occurs within the whole space or within the domain bounded by impermeable boundaries. The results obtained in this

* Correspondence to: N. P. Moshkin, School of Mathematics, Suranaree University of Technology, 111 University Avenue, Nakhon Ratchasima, 30000, Thailand.

† E-mail: moshkin@math.sut.ac.th

field are mostly local in time. The situation is completely different in two dimensions and in three dimensions. While the incompressible Euler equations in three dimensions are far from being understood, in two dimensions, the Cauchy problem for the incompressible Euler equations is much better understood. The fundamental series of works written on this subject by Perna and Majda [1, 2] include a more complete discussion of this issue.

The first theoretical result for the problem of fluid flow through a bounded domain with the impermeable, inflow, and outflow parts of the boundary was considered by Kochin [3]. He first studied the flowing-through problem in a model formulation, in which the boundary conditions at the entrance were formulated for a velocity vortex. Kazhikhov and Ragulin [4] studied the existence and uniqueness of the boundary-value problem where on the inflow parts of the boundary either three components of velocity or normal component of velocity and two tangent components of vorticity were prescribed, and on the outflow parts of the boundary either the normal component of velocity or pressure were imposed. A sufficiently full survey of works on the connection in a flowing-through problem has been provided by Antontsev *et al.* [5].

A plenty of numerical schemes have been proposed for the calculation of incompressible inviscid flows around a body or within an enclosed domain. Numerical methods for the solution of the Euler equations of an ideal incompressible fluid flow through a bounded domain with the inflow and outflow parts of boundaries have not yet been considered in detail. The present study will concentrate almost exclusively on a numerical method for the 'flowing-through' problem in which the governing equations are the steady Euler equations. The finite-difference method is based on the classical stream-function vorticity formulation of the Euler equations.

2. MATHEMATICAL FORMULATION OF FLOWING-THROUGH PROBLEMS

We present here the various kinds of well-posed flowing-through boundary-value problems for the Euler equations of an ideal incompressible fluid flow through a bounded domain. In our explanation, we follow Kazhikhov *et al.* [4].

Let Ω be a bounded domain in R^3 whose boundary Γ consists of three parts. The parts of the inflow are denoted by Γ_l^1 , and the parts of the outflow by Γ_m^2 . The part of the impermeable boundary is denoted by Γ^0 . Each component of Γ_x^i is a sufficiently smooth surface. The boundaries Γ_l^1 and Γ_m^2 do not touch each other and the intersection of Γ^0 with Γ_l^1 and Γ_m^2 occurs at the straight or right angle.

Let $\mathbf{x} = (x_1, x_2, x_3)$ denote the Cartesian co-ordinates of the points of Ω , t the time, $t \in [0, T]$, $\mathbf{u} = (u_1, u_2, u_3)$ the velocity vector, $\boldsymbol{\omega} = (\omega_1, \omega_2, \omega_3)$ the vorticity vector, P the pressure divided by the constant density of the fluid, \mathbf{f} the vector of mass forces, $Q = \Omega \times (0, T)$, $S^i = \Gamma^i \times (0, T)$, $i = 0, 1, 2$; \mathbf{n} the unit vector of the outward normal to Γ , and $\boldsymbol{\tau}_2$ and $\boldsymbol{\tau}_3$ are linearly independent vectors tangent to Γ^i , $i = 1, 2$.

The motion of a homogeneous ideal incompressible fluid is described by the Euler equations

$$\begin{aligned} \frac{\partial \mathbf{u}}{\partial t} + (\mathbf{u} \cdot \nabla) \mathbf{u} + \nabla P &= \mathbf{f} \\ \nabla \cdot \mathbf{u} &= 0, \quad (\mathbf{x}, t) \in Q \end{aligned} \quad (1)$$

At $t=0$ the velocity field is given by

$$\begin{aligned}\mathbf{u}|_{t=0} &= \mathbf{u}^0(x) \\ \nabla \cdot \mathbf{u}^0 &= 0, \quad \mathbf{x} \in \Omega\end{aligned}\quad (2)$$

A typical boundary condition on the solid parts is imposed by prescribing the value of the normal component of velocity vector as

$$(\mathbf{u} \cdot \mathbf{n}) = 0, \quad (\mathbf{x}, t) \in S^0 \quad (3)$$

and we assume that on the inflow parts of the boundary Γ_l^1 , the normal component of the velocity is given as well,

$$(\mathbf{u} \cdot \mathbf{n}) = g_l < 0, \quad (\mathbf{x}, t) \in S^1 \quad (4)$$

Additional boundary conditions must be imposed at the inflow and the outflow parts of the boundary in order to have a well-posed problem. These boundary conditions may vary. We will call the three different kinds of boundary-value problems the flowing-through problem 1, flowing-through problem 2 and flowing-through problem 3.

2.1. Flowing-through problem 1

The additional boundary conditions are the following:

Two tangent components of the vorticity vector are given on the inflow parts of the boundary S_l^1 and the normal component of the velocity vector is given on the outflow parts of the boundary S_m^2 . The whole formulation for flowing-through problem 1 is therefore as follows:

Find a solution of Equation (1) in the domain Q with initial conditions (2) and the following boundary conditions

$$\begin{aligned}S^0: \quad &(\mathbf{u} \cdot \mathbf{n}) = 0, \quad (\mathbf{x}, t) \in S^0 \\ S_l^1: \quad &(\mathbf{u} \cdot \mathbf{n}) = g_l < 0, \quad (\boldsymbol{\omega} \cdot \boldsymbol{\tau}_i) = h_i, \quad i = 2, 3, \quad (\mathbf{x}, t) \in S_l^1, \quad l = 1, 2, \dots \\ S_m^2: \quad &(\mathbf{u} \cdot \mathbf{n}) = l > 0, \quad (\mathbf{x}, t) \in S_m^2, \quad m = 1, 2, 3, \dots\end{aligned}\quad (5)$$

2.2. Flowing-through problem 2

The additional boundary conditions are the following:

Both tangent components of velocity are prescribed on the inflow parts S_l^1 and the pressure is given on S_m^2 together with a condition on the sign of the normal component of the velocity vector. The whole formulation for flowing-through problem 2 is therefore as follows:

Find a solution of Equation (1) in domain Q with initial conditions (2) and the following boundary conditions

$$\begin{aligned}S^0: \quad &(\mathbf{u} \cdot \mathbf{n}) = 0, \quad (\mathbf{x}, t) \in S^0 \\ S_l^1: \quad &(\mathbf{u} \cdot \mathbf{n}) = g_l < 0, \quad (\mathbf{u} \cdot \boldsymbol{\tau}_i) = g_i, \quad i = 2, 3, \quad (\mathbf{x}, t) \in S_l^1, \quad l = 1, 2, \dots \\ S_m^2: \quad &(\mathbf{u} \cdot \mathbf{n}) > 0; \quad P = P_2, \quad (\mathbf{x}, t) \in S_m^2, \quad m = 1, 2, 3, \dots\end{aligned}\quad (6)$$

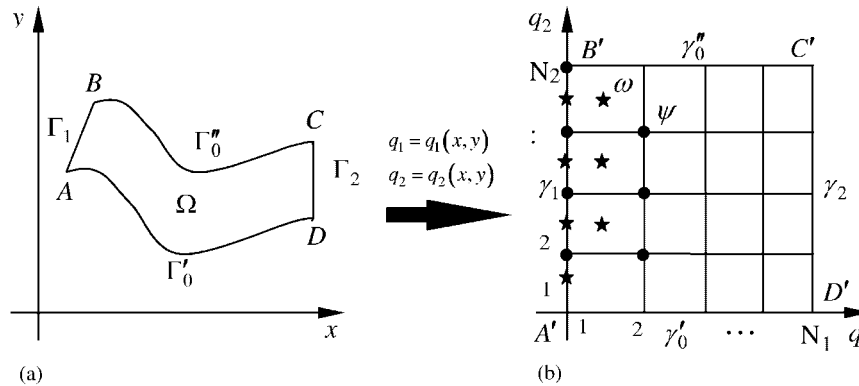


Figure 1. Physical and computational domain: (a) Physical domain; (b) Computational domain.

2.3. Flowing-through problem 3

The additional boundary conditions are the following:

Both tangent components of velocity are prescribed on the inflow parts S_l^1 and the normal component of the velocity vector is given on the outflow parts of the boundary S_m^2 . The whole formulation for flowing-through problem 3 is therefore as follows:

Find a solution of Equation (1) in domain Q with initial conditions (2) and the following boundary conditions

$$\begin{aligned}
 S^0: & \quad (\mathbf{u} \cdot \mathbf{n}) = 0, \quad (\mathbf{x}, t) \in S^0 \\
 S_l^1: & \quad (\mathbf{u} \cdot \mathbf{n}) = g_l < 0, \quad (\mathbf{u} \cdot \boldsymbol{\tau}_i) = g_i, \quad i = 2, 3, \quad (\mathbf{x}, t) \in S_l^1, \quad l = 1, 2, \dots \\
 S_m^2: & \quad (\mathbf{u} \cdot \mathbf{n}) = l > 0, \quad (\mathbf{x}, t) \in S_m^2, \quad m = 1, 2, 3, \dots
 \end{aligned}
 \tag{7}$$

3. FLOWING-THROUGH PROBLEM IN TWO-DIMENSIONAL CURVILINEAR CO-ORDINATES

The computation of flow fields in domains of complex shapes, such as shown in Figure 1(a), involves computational boundaries that do not coincide with the co-ordinate lines in the physical domain. For finite-difference methods, the formulation of boundary conditions for such problems requires interpolation of the data, and a local loss of accuracy in the computational solution will occur. These difficulties motivate the introduction of a mapping from a physical domain in the (x, y) -plane to a computational domain in curvilinear co-ordinates (q_1, q_2) . The curvilinear co-ordinates are constructed so that the computational boundaries coincide with the co-ordinate lines in the computational domain. Let

$$x = x(q_1, q_2), \quad y = y(q_1, q_2), \quad [q_1 = q_1(x, y), \quad q_2 = q_2(x, y)]
 \tag{8}$$

be a one-to-one non-singular transformation of a curvilinear domain $ABCD$ into a unit square domain $A'B'C'D'$. We assume that the inflow, the outflow and the impermeable parts Γ_i ; $i = 0, 1, 2$ of the domain boundary are transformed into γ_i ; $i = 0, 1, 2$, respectively. The boundaries $\gamma_1, \gamma_2, \gamma'_0$ and γ''_0 are the inflow, the outflow and the impermeable parts of the boundary in the computational domain (see Figure 1(b)).

We reformulate the flowing-through boundary-value problem (1), (2) and (5) in terms of the stream function and vorticity in the curvilinear co-ordinates (q_1, q_2) . The flowing-through boundary-value problem then takes the form

$$\frac{\partial}{\partial q_1} \left(Jg_{11} \frac{\partial \psi}{\partial q_1} + Jg_{12} \frac{\partial \psi}{\partial q_2} \right) + \frac{\partial}{\partial q_2} \left(Jg_{21} \frac{\partial \psi}{\partial q_1} + Jg_{22} \frac{\partial \psi}{\partial q_2} \right) = -J\omega \tag{9}$$

$$\frac{\partial}{\partial q_1} (JU_1\omega) + \frac{\partial}{\partial q_2} (JU_2\omega) = 0 \tag{10}$$

with boundary conditions on $\gamma_1, \gamma_2, \gamma'_0$ and γ''_0

$$\begin{aligned} \gamma'_0: \quad & \psi(q_1, 0) = 0 \\ \gamma''_0: \quad & \psi(q_1, 1) = c = \int_0^1 g_1(s) ds = \int_0^1 l(s) ds \\ \gamma_1: \quad & \psi(0, q_2) = \int_0^{q_2} g_1(s) ds \\ & \omega(0, q_2) = h_3(q_2) \\ \gamma_2: \quad & \psi(1, q_2) = \int_0^{q_2} l(s) ds \end{aligned} \tag{11}$$

where g_1, l, h_3 are the given values of the normal component of the velocity vector and the vorticity, respectively. Jacobian's of transformation (8), J , is not equal to zero

$$J = \frac{\partial(x, y)}{\partial(q_1, q_2)} \neq 0$$

The metric tensor components are

$$g_{ij} = \nabla q_i \cdot \nabla q_j, \quad i, j = 1, 2$$

where

$$\nabla q_i = \left\{ \frac{\partial q_i}{\partial x_1}, \frac{\partial q_i}{\partial x_2} \right\}, \quad i = 1, 2$$

The contravariant velocity components U_j in Equation (10) can be regarded as velocity components in (q_1, q_2) -space. They are

$$U_j = (\nabla \xi_j) \cdot \bar{u} \quad \left(u_i = \left(\frac{\partial x_i}{\partial \xi_j} \right) U_j \right) \tag{12}$$

The contravariant velocity components U_j can be expressed in terms of derivatives of the stream function:

$$U_1 = \frac{1}{J} \frac{\partial \psi}{\partial q_2}, \quad U_2 = -\frac{1}{J} \frac{\partial \psi}{\partial q_1} \quad (13)$$

To turn up the pressure in terms of known ψ and ω , we use the Euler equations in Gromeka–Lamb form. In curvilinear co-ordinates, they are

$$\begin{aligned} J[g_{11}U_2\omega - g_{12}U_1\omega] &= -g_{11} \frac{\partial H}{\partial q_1} - g_{12} \frac{\partial H}{\partial q_2} \\ J[g_{21}U_2\omega - g_{22}U_1\omega] &= -g_{21} \frac{\partial H}{\partial q_1} - g_{22} \frac{\partial H}{\partial q_2} \end{aligned}$$

Solving these equations with respect to $\partial H/\partial q_1$ and $\partial H/\partial q_2$ as a linear algebraic system of equations, we get

$$\begin{aligned} \frac{\partial H}{\partial q_1} &= -J\omega U_2 \\ \frac{\partial H}{\partial q_2} &= J\omega U_1 \end{aligned} \quad (14)$$

Here $H = p + |\bar{u}|^2/2$ is the total pressure and $|\bar{u}|^2 = (\bar{u} \cdot \bar{u})$ is the square of modulus of the velocity vector.

4. DISCRETIZATION OF THE EQUATIONS AND THE SOLUTION PROCEDURE

The approximated solution of problem (9)–(11) will be found by an iterative method. Let us take some initial approximations denoted by ω^0, ψ^0 . Once $\omega^{(k-1)}, \psi^{(k-1)}$; $k = 1, 2, \dots$ are known then in order to find $\omega^{(k)}, \psi^{(k)}$, we must solve the following two problems:

- (a) Determine the stream function $\psi^{(k)}(q_1, q_2)$ in terms of the vortex $\omega^{(k-1)}$ from the Poisson equation (9).
- (b) Construct a vortex field $\omega^{(k)}(q_1, q_2)$ from the Helmholtz equation (10).

In the computational domain $A'B'C'D'$, we construct a uniform rectangular finite-difference grid

$$\begin{aligned} \Omega_h &= \{[(q_1)_j, (q_2)_i], (q_1)_j = (j-1) * h_1, (q_2)_i = (i-1) * h_2 \\ & \quad i = 1, \dots, N_2; j = 1, \dots, N_1, h_1 = 1/(N_1 - 1), h_2 = 1/(N_2 - 1)\} \end{aligned}$$

The values of the stream function are approximated at the grid points. The values of the vorticity are calculated at the centre of each computational cell. At the inflow boundary $q_1 = 0$, the vorticity is evaluated at the middle point between grid nodes (see Figure 1(b)).

To find an approximate solution of the Poisson equation (9), we utilize the stabilizing correction method (see for example Reference [6]).

The stabilizing correction method consists of two steps.

The first step: We employ the implicit approximation of the partial derivative in q_1 -direction

$$\begin{aligned} \frac{\tilde{\psi}_{ij} - \psi_{ij}^{(k,s-1)}}{\Delta t} &= \left[\frac{\partial}{\partial q_1} Jg_{11} \frac{\partial \tilde{\psi}}{\partial q_1} \right]_{ij}^h + \left[\frac{\partial}{\partial q_2} Jg_{22} \frac{\partial \psi^{(k,s-1)}}{\partial q_2} \right]_{ij}^h \\ &+ \left[\frac{\partial}{\partial q_1} Jg_{12} \frac{\partial \psi^{(k,s-1)}}{\partial q_2} \right]_{ij}^h + \left[\frac{\partial}{\partial q_2} Jg_{21} \frac{\partial \psi^{(k,s-1)}}{\partial q_1} \right]_{ij}^h + J_{ij} \omega_{ij}^{(k-1)} \\ &i = 2, \dots, N_2 - 1; \quad j = 2, \dots, N_1 - 1 \end{aligned}$$

where

$$\omega_{ij} = 0.25(\omega_{i+1/2,j+1/2} + \omega_{i+1/2,j-1/2} + \omega_{i-1/2,j-1/2} + \omega_{i-1/2,j+1/2})$$

The second step: This step is a correction step and it helps to improve the stability.

$$\begin{aligned} \frac{\psi_{ij}^{(k,s)} - \tilde{\psi}_{ij}}{\Delta t} &= \left[\frac{\partial}{\partial q_2} Jg_{22} \frac{\partial \psi^{(k,s)}}{\partial q_2} \right]_{ij}^h - \left[\frac{\partial}{\partial q_2} Jg_{22} \frac{\partial \psi^{(k,s-1)}}{\partial q_2} \right]_{ij}^h \\ &i = 2, \dots, N_2 - 1; \quad j = 2, \dots, N_1 - 1; \quad s = 1, 2, \dots, S \end{aligned}$$

To approximate the partial derivatives in the square brackets, we apply the central second-order finite differences. The resulting tridiagonal system of equations is then solved by the ‘sweep method’ (see for example, Reference [6]).

As an initial guess, for $s = 1$, we set $\psi_{ij}^{(k,0)} = \psi_{ij}^{(k-1)}$. If the following convergence criteria

$$\|\psi_{ij}^{(k,S)} - \psi_{ij}^{(k,S-1)}\| \leq \varepsilon$$

is satisfied, we set $\psi_{ij}^{(k)} = \psi_{ij}^{(k,S)}$.

The integral method is used to construct the finite-difference equations for the vorticity. The equivalent integral form of Equation (10) is

$$\oint_C (JU_1 \omega \, dq_2 - JU_2 \omega \, dq_1) \equiv 0$$

where C denotes a closed curve. The contour integral is evaluated with respect to the computational cell with a central point $((q_1)_{i+1/2,j+1/2}, (q_2)_{i+1/2,j+1/2})$ (see Figure 2).

The mean value theorem is used to evaluate the integrals with respect to the cell’s sides. To represent the net flow of the vorticity through the cell’s sides, we take into account the sign of the contravariant components U_1 and U_2 of the velocity vector. In general, the values of the vorticity are determined from the finite-difference equations

$$\begin{aligned} \Lambda_1 \omega_{i+1/2,j+1/2} + \Lambda_2 \omega_{i+1/2,j+1/2} &= 0 \\ i = 1, \dots, N_2 - 1; \quad j = 1, \dots, N_1 - 1 \end{aligned} \tag{15}$$

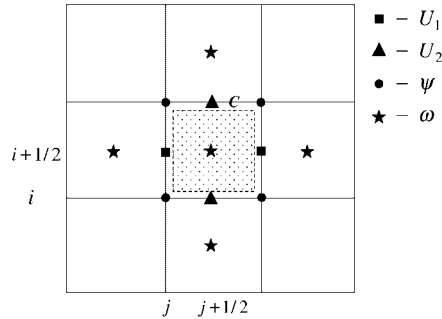


Figure 2. Stencil of the finite-difference equation.

where

$$\Lambda_1 \omega_{i+1/2, j+1/2} = \frac{1}{h_1} [(JU_1 \omega)_{i+1/2, j+1/2} - (JU_1 \omega)_{i+1/2, j}]$$

$$\Lambda_2 \omega_{i+1/2, j+1/2} = \frac{1}{h_2} [(JU_2 \omega)_{i+1/2, j+1/2} - (JU_2 \omega)_{i, j+1/2}]$$

$$\omega_{i+1/2, j} = \begin{cases} \omega_{i+1/2, j-1/2}, U_{1, i+1/2, j} \geq 0 \\ \omega_{i+1/2, j+1/2}, U_{1, i+1/2, j} < 0 \end{cases}$$

$$\omega_{i, j+1/2} = \begin{cases} \omega_{i+1/2, j+1/2}, U_{2, i, j+1/2} < 0 \\ \omega_{i-1/2, j+1/2}, U_{2, i, j+1/2} \geq 0 \end{cases}$$

It is easy to see that if we know the values of the vorticity at the grid points on the inflow part of the domain boundary then we can use the finite-difference equation (15) to find the values of the vorticity at the central point of each computational cell of the finite-difference grid Ω_h .

The iterative process is terminated when the convergence criterion is achieved

$$\max_{i, j \in \Omega_h} \left| \frac{\omega_{ij}^{(n)} - \omega_{ij}^{(n-1)}}{\omega_{ij}^{(n)}} \right| < \varepsilon_\omega, \quad \max_{i, j \in \Omega_h} \left| \frac{\psi_{ij}^{(n)} - \psi_{ij}^{(n-1)}}{\psi_{ij}^{(n)}} \right| < \varepsilon_\psi$$

where ε_ω and ε_ψ are the convergence tolerances.

5. CONVERGENCE

A test problems with known analytical solution are chosen to demonstrate the convergence of the finite-difference scheme presented in the previous section. A rigorous comparison of the approximate and exact solutions was performed.

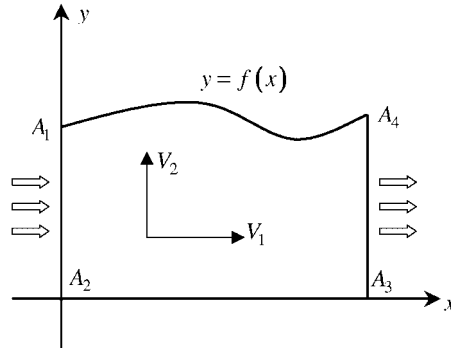


Figure 3. Flow domain of the test problem.

To construct a test problems with known analytical solution, we use the results of Alekseev *et al.* [7]. This work has been published in local Russian journal and access to it is difficult. We will give a more detailed description of exact solutions reduced from above mentioned article. The flow domain Ω is a plane channel $A_1A_2A_3A_4$ with one curved wall A_1A_4 (see Figure 3). The equation of curved wall is $y = f(x)$ and this function is a solution of

$$\frac{d^2 f(x)}{dx^2} = c f(x) \tag{16}$$

where c is an arbitrary constant. Additionally, $f(x)$ has to satisfy the requirements

$$\begin{aligned} f(0) &= b \\ f(x) &> 0, \quad x \in [0, a] \\ f(x) \cdot \frac{d^2 f(x)}{dx^2} - \left(\frac{df(x)}{dx} \right)^2 &= c_1 < 1 \end{aligned} \tag{17}$$

where c_1 is a constant. Than, for an arbitrary constant $c_2 > 0$, the solution of the Euler equations in plane channel $A_1A_2A_3A_4$ has the form

$$\begin{aligned} v_1(x, y) &= \frac{c_2 f(x)}{f^2(x) - c_1 y^2} \\ v_2(x, y) &= \frac{c_2 y f'(x)}{f^2(x) - c_1 y^2} \\ P(x, y) &= P_0 - \frac{\rho c_2^2}{2(f^2(x) - c_1 y^2)} \end{aligned} \tag{18}$$

where P_0 is an arbitrary constant. From formulas (18), we can find the vorticity and the Bernoulli function,

$$\omega(x, y) = -cc_2 y f(x) \frac{f^2(x) + c_1 y^2}{(f^2(x) - c_1 y^2)}$$

$$H(x, y) = \frac{P_0}{\rho} + cc_2^2 \frac{y^2 f^2(x)}{2(f^2(x) - c_1 y^2)^2}$$

If $c_1 = -\sigma^2 < 0$ then, by using Equation (18), it is easy to find formulas for the stream function and vorticity,

$$\psi(x, y) = \frac{c_2}{\sigma} \arctan \frac{\sigma y}{f(x)}$$

$$\Delta\psi = -\frac{cc_2}{4\sigma} \sin\left(\frac{4\sigma}{c_2} \psi\right)$$

The general solution of Equation (16) for $c < 0$ is well known,

$$f(x) = K_1 e^{i\sqrt{c}x} + K_2 e^{-i\sqrt{c}x}$$

where $i^2 = -1$ and the constants K_1 and K_2 have to be real and satisfy the non-linear system due to requirements (17)

$$-4cK_1K_2 = c_1$$

$$K_1 + K_2 = b$$

In the particular case when

$$c = \left(\frac{\sigma}{b}\right)^2$$

it follows that

$$f(x) = b \cos \frac{|\sigma|}{b} x, \quad x \in [0, a], \quad a < \frac{\pi}{2} \frac{b}{|\sigma|} \quad (19)$$

We consider the test problem with parameters

$$\sigma = 1, \quad b = 1, \quad c_2 = 4, \quad a = 0.5$$

For this set of parameters, the analytical solution of the Euler equations is

$$f(x) = \cos(x)$$

$$\psi(x, y) = 4 \arctan\left(\frac{y}{\cos(x)}\right) \quad (20)$$

$$\omega(x, y) = \sin(\psi(x, y))$$

Table I. Absolute errors of stream function and vorticity and rate of convergence for test problem (20).

Grid $N_1 \times N_2$	$\ \psi^h - \psi\ _\infty \times 10^5$	Rate of converg. (25)	$\ \omega^h - \omega\ _\infty \times 10^5$	Rate of converg. (25)
11 × 11	5.52	—	4.75	—
21 × 21	1.03	2.41	1.20	1.97
41 × 41	0.25	2.00	0.31	1.92

If $0 < c_1 = \sigma^2 < 1$ then the formulas for the stream function and vorticity are

$$\psi(x, y) = \frac{c_2}{2\sigma} \ln \frac{f(x) + \sigma y}{f(x) - \sigma y} \tag{21}$$

$$\Delta\psi = \frac{cc_2}{4\sigma} \sinh\left(\frac{4\sigma}{c_2} \psi\right) \tag{22}$$

In a particular case where

$$b^2 = \frac{\sigma^2}{c}$$

the equation of curve wall is

$$f(x) = b \cosh(\sqrt{c}x), \quad x \in [0, a] \tag{23}$$

In this case we have a divergent channel. For particular values of parameters

$$\sigma = 0.5, \quad a = 1, \quad b = 1, \quad c_2 = 1, \quad c = c_1 = \sigma^2 = 0.25$$

the analytical solution (21), (22) and (23) is the following:

$$\begin{aligned} f(x) &= \cosh(0.5x) \\ \psi(x, y) &= \ln\left(\frac{\cosh(0.5x) + 0.5y}{\cosh(0.5x) - 0.5y}\right) \\ \omega(x, y) &= 0.125 \sinh(2\psi(x, y)) \end{aligned} \tag{24}$$

The algorithm developed in Section 4 is then implemented to these test problems. Tables I and II show the infinity norm of absolute errors which are obtained from grid systems having 11 × 11, 21 × 21 and 41 × 41 nodes. With these values, the resulting rate of convergence is estimated. The rate of convergence is defined as follows:

$$m = \frac{1}{\ln(N_2/N_1)} \ln\left(\frac{\text{err } 1}{\text{err } 2}\right) \tag{25}$$

where err 1 and err 2 are errors which correspond to grid systems with $N_1 \times N_1$ and $N_2 \times N_2$ nodes, respectively. It is observed that the convergence rate is approximately equal to two. This confirms that the finite-difference scheme is of second-order accuracy.

Table II. Absolute errors of stream function and vorticity and rate of convergence for test problem (24).

Grid $N_1 \times N_2$	$\ \psi^h - \psi\ _\infty \times 10^5$	Rate of converg. (25)	$\ \omega^h - \omega\ _\infty \times 10^5$	Rate of converg. (25)
11 \times 11	2.82	—	1.45	—
21 \times 21	0.47	2.58	0.38	1.93
41 \times 41	0.10	2.23	0.11	1.79

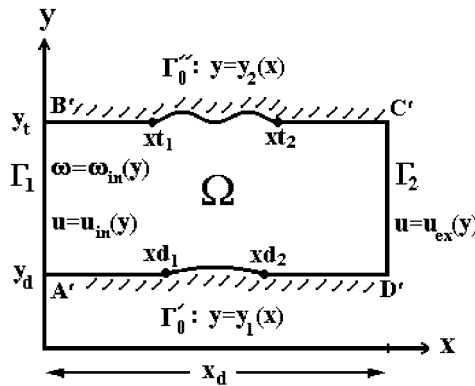


Figure 4. Sketch of channel with curved walls.

6. NUMERICAL RESULTS FOR A FLOW THROUGH A CHANNEL WITH CURVED WALLS

The numerical method developed in Section 4 will now be applied to study the internal flow of an ideal incompressible fluid in a two-dimensional channel with curved walls. The channel geometry and boundary conditions are shown in Figure 4. The equations of the impermeable walls Γ_0', Γ_0'' are

$$y_i(x) = \begin{cases} y_\alpha & ; 0 < x < x\alpha_1 \\ y_\alpha + h_\alpha [1 + \sin z(x)] & ; x\alpha_1 \leq x \leq x\alpha_2, \quad i = 1, 2 \\ y_\alpha & ; x\alpha_2 < x < 0 \end{cases} \quad (26)$$

where $\alpha = d$ in the case of the lower boundary and $\alpha = t$ in the case of the top boundary of channel. The function $z(x)$ is defined by the equation

$$z(x) = \frac{\pi}{2(x\alpha_2 - x\alpha_1)} [2(K_\alpha + 1)x - (2K_\alpha + 1)x\alpha_1 - x\alpha_2], \quad K_\alpha = 1, 3, 5 \dots \quad (27)$$

The number of troughs and crests of the boundary in the interval $(x\alpha_1, x\alpha_2)$ will be determined by the choice of K_α in Equation (27). The value h_α determines the vertical sizes of troughs

and crests. The normal component of the velocity vector and vorticity are specified at the inflow part of boundary Γ_1 :

$$U_{1in}(y) = C_{in} = \text{const} \quad (28)$$

$$\omega_{in}(y) = a_{\omega} \sin\left(K \frac{y - y_d}{y_t - y_d} \pi\right); \quad K = 1, 2, \dots \quad (29)$$

The impermeable boundaries, Γ_0' and Γ_0'' are enforced by the condition $\vec{u} \cdot \vec{n} = 0$. The normal component of the velocity vector is specified at the outflow part boundary Γ_2 :

$$U_{1out}(y) = C_{out} = \text{const}$$

The parameters C_{in} , C_{out} and K are chosen so that the consistency of boundary conditions holds

$$\omega_{in}(y_d) = - \left. \frac{\partial U_1}{\partial y} \right|_{y=y_d}; \quad \omega_{in}(y_t) = - \left. \frac{\partial U_1}{\partial y} \right|_{y=y_t}$$

We point out that all the results presented hereafter were computed on the PC with AMD Athlon(TM) Processor, 1.0GHz. Microsoft Fortran was used to developed computer code. All computations were performed for the rectangular uniform grid in the computational domain. A mesh sensitivity was carried out by halving the grid size in both directions. In all cases the relative difference between solutions was smaller then 5% in the uniform norm. Therefore, the solutions presented here are considered grid independent. Grids of 41×41 nodes provide good resolution. Several computations with 81×81 nodes were done to verify this. To get the convergence of general iterative process it was need 50–100 iterations. The inner iterative process for stream function converged for 1–5 iterations. Computational time required for 50 iterations approximately equal 0.3 s.

Figures 5–8 illustrate the distribution of the pressure field and the streamlines for various boundary conditions for vorticity at the entrance. Boundary conditions for vorticity at the inflow part of boundary are prescribed by Equation (29). The geometry of the walls is given by Equation (26) and parameters are equal to $y_d = 0$, $y_t = 1$, $xt_1 = 1.0$, $xt_2 = 2.0$, $xd_1 = 1.5$, $xd_2 = 2.5$, $h_t = -0.1$ and $h_d = 0.1$. The total length of channel x_d is 4.0. The transformation of the physical domain into the computational domain is given in the following form:

$$q_1 = \frac{x}{x_d}, \quad q_2 = \frac{y - y_1(x)}{y_2(x) - y_1(x)}$$

Figures 5(a)–5(d) show the pressure contours for various parameters. Figure 5(a) corresponds to the potential flow (the vorticity at the inflow boundary vanishes, $a_{\omega} = 0$). Figures 5(b) and 5(c) correspond to the cases where $K = 1.0$ in Equation (29). In these two cases the vorticity does not change sign at the entrance and has amplitudes $a_{\omega} = 1.0$ and 5.0, respectively. Figure 5(d) corresponds to the case $a_{\omega} = 5.0$, $K = 2.0$. In this case the vorticity at the entrance has positive and negative values with amplitude $a_{\omega} = 5.0$. The values of the isolines in Figures 5(a) and 5(b) vary from -1.4 to -0.1 with an interval of 0.1. In Figures 5(c) and 5(d), only seven isolines which are equally distributed between maximal and minimal values of the pressure field are drawn.

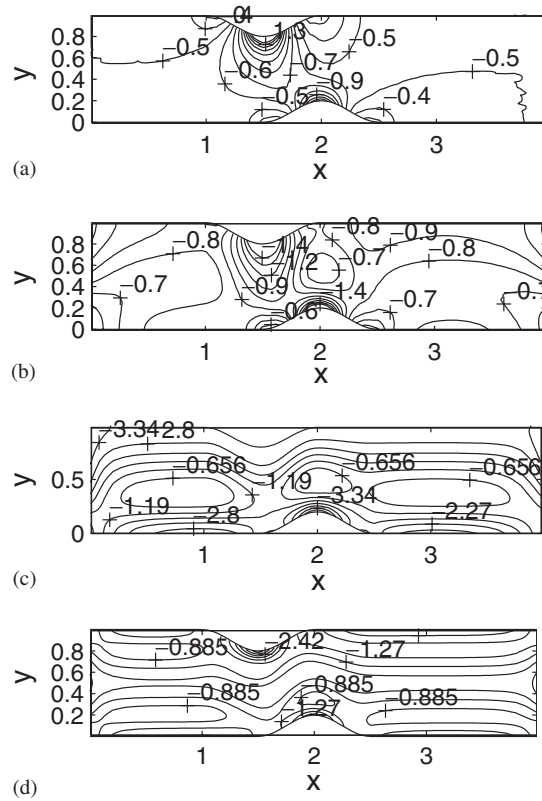


Figure 5. Pressure contours for: (a) $a_\omega = 0.0$, $K = 1.0$; (b) $a_\omega = 1.0$, $K = 1.0$; (c) $a_\omega = 5.0$, $K = 1.0$; (d) $a_\omega = 5$, $K = 2$.

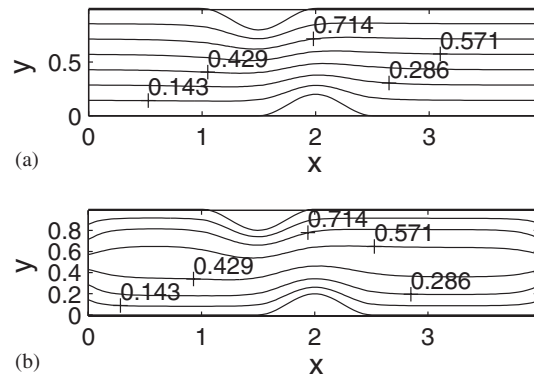


Figure 6. Stream function for: (a) $a_\omega = 0.0$, $K = 1.0$; (b) $a_\omega = 5$, $K = 2$.

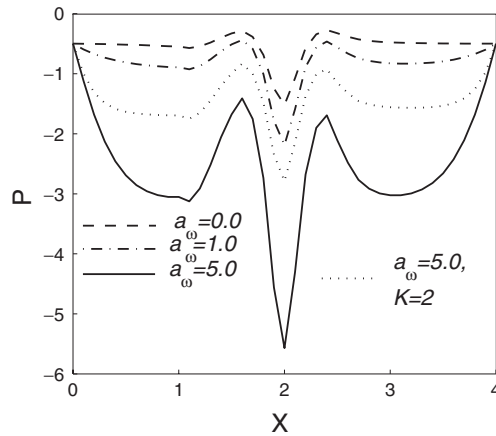


Figure 7. Pressure along lower boundary.

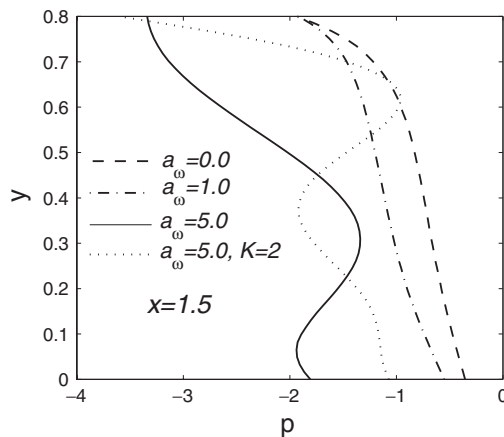


Figure 8. Pressure at the section $x = 1.5$.

Figures 6(a)–6(b) illustrate the streamlines (or trajectories) of fluid flow within the channel. Figure 6(a) corresponds to the potential flow where $a_\omega = 0.0$. Figures 6(b) corresponds to the case $a_\omega = 5.0$, $K = 2.0$. It is clear that the non-zero value of vorticity at the entrance corresponds to a non-zero angle between the direction of the inlet velocity vector and the direction of the Ox -axis.

The pressure along the lower boundary as a function of x is shown in Figure 7. The values of K and a_ω vary as indicated in Figure 7. The results for the case $a_\omega = 0$ are plotted by the dashed line. The dash-dotted lines in Figure 7 represents the pressure for the case $a_\omega = 1.0$. The solid line represents the pressure for the case $a_\omega = 5.0$. The dotted line represents the pressure for the case $a_\omega = 5.0, K = 2$. The absolute values of the pressure peaks near the points $x = 1.0$, 1.5 and 2.0 increase together with increasing magnitude a_ω , of the vorticity given

at the entrance. Also, we can observe the decrease of the pressure peaks near the points $x = 1.0, 1.5$ and 2.0 with increasing values of the parameter K , from 1.0 to 2.0 .

Figure 8 illustrates the behaviour of the pressure at the section $x = 1.5$ for different boundary conditions for the vorticity. Figure 8 demonstrates the function

$$P = P(x, y)|_{x=1.5} \quad (30)$$

for four different values of a_ω and K in Equation (29). The dashed line in Figure 8 corresponds to the case $a_\omega = 0$ which represents the potential flow. The dash-dotted line represents the function (30) for the case $a_\omega = 1.0$. The solid line shows the result for the case $a_\omega = 5.0$. The dotted line shows the result for the case $a_\omega = 5.0, K = 2$. In the case $a_\omega = 5.0$, function (30) has several local extreme. In the case $K = 2.0$, we can observe that the number of local extremes increases compared with case where $K = 1$.

7. CONCLUSIONS

The finite-difference algorithm is constructed for the steady two-dimensional ‘flowing-through’ problem in which the governing equations are the inviscid Euler equations. This algorithm is essential for boundary-value problems in which at the inflow parts of boundary, the normal component of the velocity vector and the tangent components of the vorticity are given, and on the outflow parts, only the normal component of the velocity vector is known. The values of the normal component of velocity are given on the impermeable boundaries.

The vorticity and the stream-function form of the Euler equations has been exploited to construct the numerical algorithm. Algebraic mapping techniques with one-dimensional stretching functions are used to establish the correspondence between points in the irregular physical domain and points in the regular computational domain. The algebraic equations produced by discretising the Euler equations in vorticity, stream function form are essentially non-linear for vortical flow. The appropriate iterative process is suggested. An outer iteration decouples the Poisson equation for the stream function and the Helmholtz equation for vorticity. At each step of the outer iteration, a linear system of equations is solved by the stabilizing correction method. The Helmholtz equation for vorticity has hyperbolic character. The marching algorithm based on upwind approximation of convective terms is applied to obtain the downstream development of the vorticity field.

The convergence of the numerical algorithm is confirmed by a test problem with known analytical solution. Numerical calculations are performed for the two-dimensional inviscid flow through a channel with curved walls. The proposed schemes are confirmed to be efficient for a wide range of parameters. Strong dependence of the pressure field on the boundary conditions for the vorticity is shown.

REFERENCES

1. Di Perna RJ, Majda A. Concentration in regularizations for 2D incompressible flow. *Communications on Pure and Applied Mathematics* 1987; **40**:511–547.
2. Di Perna RJ, Majda A. Reduced Hausdorff dimension and concentration cancelation for 2-D incompressible flow. *Journal of the American Mathematical Society* 1988; **1**:59–96.
3. Kochin NE. On one existence theorem in hydrodynamics. *Prikladnaya matematika i mekh* 1956; **20**(2): 153–172 (Translated in *Journal of Applied Mathematics and Mechanics* ISSN 0021-8928).

4. Kazhikhov AV, Ragulin VV. Nonstationary problems on ideal fluid flow through the bounded domain. *Doklady Akademi Nauk USSR* 1980; **250**(6):1344–1347.
5. Antontsev SN, Kazhikhov AV, Monakhov VN. *Boundary Value Problems in Mechanics of Nonhomogeneous Fluids*. Netherlands, 1990.
6. Yanenko NN. *The Method of Fractional Steps: The Solution of Problems of Mathematical Physics in Several Variables*. Springer: New York, Berlin, Heidelberg, 1971.
7. Alekseev GV, Mokin YA. *Dinamika Sploshnoi Sredu* 1972; **12**:5–13.